

Mesoscopic fluctuations in biharmonically driven flux qubits

Alejandro Ferrón

Instituto de Modelado e Innovación Tecnológica (CONICET-UNNE) and Facultad de Ciencias Exactas, Naturales y Agrimensura, Universidad Nacional del Nordeste, Avenida Libertad 5400, W3404AAS Corrientes, Argentina

Daniel Domínguez and María José Sánchez

Centro Atómico Bariloche and Instituto Balseiro, 8400 San Carlos de Bariloche, Argentina

(Received 25 October 2016; revised manuscript received 29 December 2016; published 17 January 2017)

We investigate flux qubits driven by a biharmonic magnetic signal, with a phase lag that acts as an effective time reversal broken parameter. The driving induced transition rate between the ground and the excited state of the flux qubit can be thought of as an effective transmittance, profiting from a direct analogy between interference effects at avoided level crossings and scattering events in disordered electronic systems. For time scales prior to full relaxation, but large compared to the decoherence time, this characteristic rate has been accessed experimentally by Gustavsson *et al.* [*Phys. Rev. Lett.* **110**, 016603 (2013)] and its sensitivity with both the phase lag and the dc flux detuning explored. In this way, signatures of universal conductance fluctuationslike effects have been analyzed and compared with predictions from a phenomenological model that only accounts for decoherence, as a classical noise. Here we go beyond the classical noise model and solve the full dynamics of the driven flux qubit in contact with a quantum bath employing the Floquet-Born-Markov master equation. Within this formalism, the computed relaxation and decoherence rates turn out to be strongly dependent on both the phase lag and the dc flux detuning. Consequently, the associated pattern of fluctuations in the characteristic rates display important differences with those obtained within the mentioned phenomenological model. In particular, we demonstrate the weak localizationlike effect in the average values of the relaxation rate. Our predictions can be tested for accessible but longer time scales than the current experimental times.

DOI: [10.1103/PhysRevB.95.045412](https://doi.org/10.1103/PhysRevB.95.045412)**I. INTRODUCTION**

The quantum conductance of a phase coherent conductor can be related, in the diffusive regime, to the transmission probability through the disordered region [1]. For milli-Kelvin temperatures, when typically the coherence length could become larger than the scattering mean free path, the interference term present in the transmission probability survives disordered averaging, giving rise to quantum corrections to the classical transport properties and novel phenomena. Mesoscopic effects like weak localization and universal conductance fluctuations have been predicted and extensively tested in electronic quantum systems for years [2–4].

Universal conductance fluctuations (UCFs) are sample to sample fluctuations—of the order of the quantum of conductance—originated on the sensitivity of the quantum conductance to changes in an external parameter, like a magnetic flux or a gate voltage [2].

The weak localization (WL) effect is a quantum correction to the classical conductance that survives disorder averaging when time reversal symmetry is present [3]. Without spin-orbit effects, it is characterized by a dip in the conductance (peak in the resistance) at zero magnetic field. The standard way to detect the WL effect is by its suppression, as its strength falls off with an applied magnetic field. A critical field that scales as $B_c \sim 1/(D\tau_\phi)$, with D the diffusion coefficient and τ_ϕ the coherence time, washes out the quantum interference term, and thus the WL correction [3]. The measurement of B_c has been established as a usual route to determine the coherence time [3,4].

Flux qubits (FQs) are model artificial atoms whose energy levels can be manipulated by an external magnetic flux [5–9].

For most of the applications in quantum information theory, only the two lowest energy levels have been considered in studies of their quantum dynamics [6]. However, FQs exhibit as a function of the static magnetic flux a complex structure of energy levels with multiple avoided crossings. This rich spectrum can be explored by driving the FQs with an ac magnetic flux, for moderate driving frequencies—in the microwave range. In a typical protocol, FQs are initially prepared in the ground state for a given value of the dc flux, evolving under the ac driving quasiadiabatically until the first avoided crossing is reached. There the state obeys a Landau-Zener-Stückelberg (LZS) transition and transforms into a coherent superposition of the ground and excited states [10,11]. For weak ac amplitudes, such that a single avoided crossing is reached by the driving protocol, the superposition state and the initial one interfere again at the second passage for the avoided crossing. Hence, the avoided crossing acts as an effective beam splitter, where scattering events take place. For driving periods larger than the coherence time, the evolved state accumulates a total phase that depends both on the dc flux and the driving amplitude [10,11].

The regime of weak driving (small amplitudes), when only the lowest two energy levels of the FQs are explored and a single avoided crossing is attained by the amplitude of the ac flux, has been studied both experimentally and theoretically [10,12,13]. In this way, FQs have been investigated extensively in recent years as high resolution Mach-Zehnder type of interferometers [10].

For large driving amplitudes, when many avoided crossings can be reached, the repeated sweeps through the avoided level crossings result in successive LZS transitions between different energy levels. This driving protocol—named as

amplitude spectroscopy [10]—was employed to reconstruct the FQs energy level spectra and to study the dynamics under different conditions [14,15]. It has been also successfully applied in other systems like charge qubits [16], ultracold molecular gases [17], and single electron spins [18].

The interaction of driven FQs with an external bath has been recently studied to incorporate more realistic dissipative scenarios beyond the pure coherent regime. Relevant and potential useful phenomena like population inversion [19–21], dynamical transition in the interference patterns [22], and estimates for coherence times have been extracted from these studies [23,24].

While *a priori* there is not a direct connection between driven FQs and mesoscopic disordered electronic systems, the identification of a transition at an avoided crossing as a scattering event, suggests a route to study mesoscopiclike effects in driven FQs.

However, for an harmonic protocol in the weak driving regime, only one avoided crossing is traversed back and forth in one period of the signal. Consequently, the qubit experiences two scattering events (transitions) over a single period and only one relative phase (that controls the interference between the initial and the superposition states) is accumulated during the evolution [10]. Notice that this is a poor scattering regime which seems insufficient to explore the mesoscopic analogy.

An alternative to go beyond this limitation, in order to increase the number of scattering events but within the weak driving regime, was proposed in Ref. [12] with the implementation of a protocol generated by a biharmonic flux with a phase lag. The signal was designed to drive the qubit up to four times through the avoided crossing in one period, which was chosen as much shorter than the energy relaxation time. Therefore, after many periods of driving, the excited state of the qubit was populated as a function of time with a characteristic (equilibration) rate that was extracted in the experiment by a fitting procedure.

The key point is that for a nonzero phase lag, the biharmonic signal turns asymmetric in time and three different phases can be accumulated per cycle of driving. These phases, which rule the interference conditions, can be changed by either tuning the external dc flux or the phase lag in the driving wave form. Following this strategy, the equilibration rate Γ and its concomitant fluctuations have been analyzed in Ref. [12]. The fluctuations in Γ have been interpreted as interference between all possible paths generated by the total number of scattering events, which is ultimately set by the coherence time of the FQs.

For large driving frequencies and for time scales smaller than the relaxation time but larger than the decoherence time, it is possible to study the dynamics of the FQs within a model of classical diagonal noise and computing Γ from phenomenological rate equations [25]. Neglecting relaxation, it can be shown that $\Gamma \sim 2W$, with W the transition rate induced by driving [25]. The mesoscopic analogy proposed in Ref. [12] was to identify W with a transmission rate, which in (mesoscopic) electronic transport determines the conductance [1]. Thus the goal was to access the fluctuations in W through the study of the fluctuations in Γ . This scenario, although tempting, should be taken with caution.

As we already mentioned, the expression $\Gamma \sim 2W$ is valid for large driving frequencies and for time scales far below relaxation [12,26]. Here we go beyond these assumptions, and solve the full dynamics of the driven FQs employing the Floquet-Born-Markov master equation to include relaxation and decoherence processes for a realistic model of a quantum bath [20–22]. This formalism [27], valid for arbitrary time scales and strength of the driving protocol, allows us to compute the decoherence and the relaxation (equilibration) rates. As we will show, both rates turn out to be strongly dependent on the driving amplitude and the dc flux, attaining values that might differ up to an order of magnitude from those determined in the absence of driving. Consequently, the relaxation (equilibration) rate obtained within the FM formulation might strongly differ from the value $2W$ —used in Ref. [12] to compare with the experimental results.

An important outcome of our study is the prediction of the WL effect, which was not resolved in the experiment of Ref. [12]. As we will analyze, it is not the driving protocol but the accessible decoherence time which limits the detection of the effect [12]. In fact, the WL correction could be measured in the regime of larger coherence times.

The paper is organized as follows. In Sec. II we review the Hamiltonian model for the FQs and the effective Hamiltonian obtained when only the two lowest levels are considered. In Sec. III A we derive an analytical expression for the rate Γ , employing a phenomenological approach which includes classical noise as the only source of decoherence [25]. Gaussian and low frequency types of noise are both considered [28].

Due to the limitations of the analytical approach already mentioned, we implement in Sec. III B the full quantum mechanical calculation in order to obtain the equilibration (relaxation) rate Γ_r within the Floquet-Born-Markov master equation. The last part of this section is devoted to compare the behavior of $\Gamma \sim 2W$ and Γ_r as a function of the dc flux, and to analyze the effect that the driving has on the determination of the decoherence and relaxation rates. The fluctuations in the rates $\Gamma \sim 2W$ and Γ_r as a function of the dc flux and the time reversal parameter are analyzed in Sec. IV. As we show, besides UCF, clear signatures of WL correction could be also detected if the coherence is increased. We discuss the limitation imposed by the accessible decoherence time in the experimental determination of the WL correction. We conclude in Sec. V with a discussion and perspectives.

II. THE HAMILTONIAN MODEL FOR THE FQs

The FQs consist of a superconducting ring with three Josephson junctions [5] enclosing a magnetic flux $\Phi = f\Phi_0$, with $\Phi_0 = h/2e$. Two of the junctions have the same Josephson coupling energy $E_{J,1} = E_{J,2} = E_J$ and capacitance $C_1 = C_2 = C$, while the third one has smaller coupling $E_{J,3} = \delta E_J$ and capacitance $C_3 = \delta C$, with $0.5 < \delta < 1$. The junctions have gauge invariant phase differences defined as φ_1 , φ_2 , and φ_3 , respectively. Typically the circuit inductance can be neglected and the phase difference of the third junction is $\varphi_3 = -\varphi_1 + \varphi_2 - 2\pi f$.

Therefore, the system can be described in terms of two independent dynamical variables, chosen as $\varphi_l = (\varphi_1 - \varphi_2)/2$ (longitudinal phase) and $\varphi_t = (\varphi_1 + \varphi_2)/2$ (transverse phase).

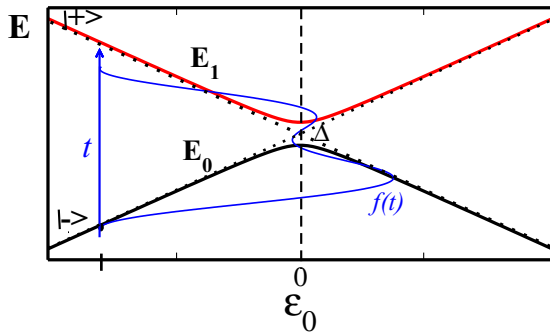


FIG. 1. Energy diagram for the TLS Hamiltonian Eq. (2), as a function of flux detuning ε_0 . Inset: Implemented biharmonic pulse $f(t)$, chosen to drive the TLS four times through the avoided crossing in one period.

In terms of these variables, the Hamiltonian (in units of E_J) is [5]

$$\mathcal{H}_{\text{FQ}} = -\frac{\eta^2}{4} \left(\frac{\partial^2}{\partial \varphi_l^2} + \frac{1}{1+2\delta} \frac{\partial^2}{\partial \varphi_t^2} \right) + V(\varphi_l, \varphi_t), \quad (1)$$

with $\eta^2 = 8E_C/E_J$ and $E_C = e^2/2C$. The kinetic term corresponds to the electrostatic energy of the system and the potential one to the Josephson energy of the junctions, given by $V(\varphi_l, \varphi_t) = 2 + \delta - 2 \cos \varphi_l \cos \varphi_t - \delta \cos(2\pi f + 2\varphi_l)$. Typical experiments have values of δ in the range 0.6–0.9 and η in the range 0.1–0.6 [6,14]. FQs are operated at magnetic fields near the half-flux quantum [5,6] $f = 1/2 + f_0$, with $f_0 \ll 1$. For $\delta \geq 1/2$, the potential $V(\varphi_l, \varphi_t)$ has two minima at $(\varphi_l, \varphi_t) = (\pm\varphi^*, 0)$ separated by a maximum at $(\varphi_l, \varphi_t) = (0, 0)$. Each minima corresponds to macroscopic persistent currents of opposite sign, and for $f \gtrsim 1/2$ ($f \lesssim 1/2$) a ground state $|+\rangle$ ($|-\rangle$) with positive (negative) loop current is favored.

For values of $|f_0| \ll 1$, such that the avoided crossings with the third energy level are not reached, the Hamiltonian of Eq. (1) can be reduced to the two-level system (TLS) [5,13]

$$\mathcal{H} = -\frac{\varepsilon_0}{2} \hat{\sigma}_z - \frac{\Delta}{2} \hat{\sigma}_x, \quad (2)$$

in the basis defined by the persistent current states $|\pm\rangle = (|0\rangle \pm |1\rangle)/\sqrt{2}$, with $\hat{\sigma}_z, \hat{\sigma}_x$ the Pauli matrices and $|0\rangle$ and $|1\rangle$ the ground and excited states at $f_0 = 0$. The parameters of \mathcal{H} are the gap (at $f_0 = 0$) Δ and the detuning energy $\varepsilon_0 = 4\pi I_p f_0$. Here $I_p = \delta|\langle +|\sin 2\varphi_l|+\rangle| = \delta|\langle -|\sin 2\varphi_l|-\rangle|$ is the magnitude of the loop current, which for our case with $\delta = 0.8$ and $\eta = 0.25$ is $I_p = 0.721$ (in units of $I_c = 2\pi E_J/\Phi_0$).

Figure 1 sketches the energy levels diagram for the Hamiltonian restricted to the TLS, Eq. (2) with $E_{0,1} = \pm 1/2 \sqrt{\varepsilon_0^2 + \Delta^2}$ as the ground and excited states energies, respectively [10,14,26].

FQs restricted to weak driving amplitudes were the regime explored in Ref. [12]. Consistently, in the following we focus on the dynamics of the TLS Hamiltonian Eq. (2) under the effect of the biharmonic driving.

III. TWO-LEVEL SYSTEM UNDER BIHARMONIC DRIVING

A. Equilibration rate within the classical noise model

As we mentioned, in Ref. [12] the equilibration rate Γ is experimentally determined by fitting the decay of the excited population to the equilibrium, assuming an exponential behavior as a function of time.

In the following we describe a route to compute Γ from phenomenological rate equations in the regime of large driving frequencies, for which the change in the qubit population (per unit time) induced by the driving is small compared to the decoherence rate $\Gamma_2 \equiv 1/T_2$ but large compared to the inelastic relaxation rate in the absence of driving $\Gamma_1 \equiv 1/T_1$. As the calculation is adapted from the one derived for the single driving protocol [26], here we present the main steps stressing differences. The source of noise is considered classical and diagonal, which essentially means that the noise produces pure dephasing. However, diagonal noise is consistent with the typical experimental situation with FQs where the dominant source of noise is fluxlike.

From phenomenological rate equations the equilibration rate can be written as $\Gamma = 2W + \Gamma_1$, with W the transition rate induced by the driving protocol [26]. For large relaxation times T_1 and for $W \gg \Gamma_1$, one gets $\Gamma \approx 2W$. Larger values of Γ_1 would require the explicit inclusion of relaxation processes in the analysis to avoid important differences between $2W$ and Γ . These cases will be addressed in Sec. III B.

To compute W , we include in Eq. (2) the time dependent biharmonic driving and the diagonal classical noise by replacing $\varepsilon_0 \rightarrow h(t) = \varepsilon_0 + \delta\varepsilon + \varepsilon(t)$. The term $\varepsilon(t) = 4\pi I_p f(t)$ contains the biharmonic ac flux $f(t) = A_1 \cos(\omega_0 t + \alpha) - A_2 \cos(2\omega_0 t)$ of fundamental frequency $\omega_0 = 2\pi/\tau$. The phase lag α turns the protocol asymmetric in time and the amplitudes ratio A_1/A_2 was chosen to drive the qubit up to four times through the avoided crossing in one period τ . The classical noise is $\delta\varepsilon$.

After an unitary transformation $\exp[i\phi(t)\hat{\sigma}_z]$ with $\phi(t) = \int_0^t h(t') dt'$, the Hamiltonian Eq. (2) can be turned to purely off-diagonal (we use $\hbar = 1$)

$$\tilde{\mathcal{H}} = -\frac{\Delta^*(t)}{2} \hat{\sigma}_x,$$

where $\Delta(t) = \Delta e^{-i\phi(t)}$ and $\phi(t) = \int_0^t h(t') dt'$.

The system is usually initially prepared in its ground state $|\Psi_g(t=0)\rangle$ for a given value of the detuning ε_0 (in Fig. 1 an initial state for $\varepsilon_0 < 0$ is chosen). Alternatively, it is possible to initialize the FQs in an eigenstate of the computational basis, i.e., $|-\rangle$ ($|+\rangle$) for $\varepsilon_0 < 0$ ($\varepsilon_0 > 0$). In general, for values of flux detuning $\varepsilon_0 > \Delta$, the initial state satisfies $|\Psi_g(t=0)\rangle \rightarrow |-\rangle(|+\rangle)$ for $\varepsilon_0 < 0$ ($\varepsilon_0 > 0$).

The transition rate W induced by the driving is the time derivative of the transition probability between the initial and the final state. Under the assumption of fast driving, $\omega_0 = 2\pi/\tau > \Delta$, it can be computed expanding the time evolution operator to first order in Δ ,

$$U(t,0) = 1 - i \int_0^t \tilde{\mathcal{H}}(\tau) d\tau + O(\Delta^2).$$

Therefore we write

$$\begin{aligned}
 W &= \frac{d}{dt} | \langle + | U(t,0) | - \rangle |^2 = \frac{d}{dt} \frac{1}{4} \int_0^t \int_0^t \Delta(\tau_1) \Delta^*(\tau_2) d\tau_1 d\tau_2 \\
 &= \frac{d}{dt} \frac{\Delta^2}{4} \int_0^t \int_0^t \text{Re} \{ \exp -i[\phi(\tau_1) - \phi(\tau_2)] \} d\tau_1 d\tau_2, \quad (3)
 \end{aligned}$$

with $\text{Re}\{\dots\}$ the real part.

In the above integrand we define

$$e^{-i\phi(t)} = e^{-i\varepsilon_0 t - i\delta\phi(t)} \sum_{nm} J_n(x_1) e^{in(\omega_0 t + \alpha)} J_m(x_2) e^{-i2m\omega_0 t}, \quad (4)$$

where we have used the expansion of $\exp(ix \sin u) = \sum_p J_p(x) \exp(-ipu)$ in terms of Bessel functions of first kind. We also defined $x_1 = A_1/\omega_0$ and $x_2 = A_2/(2\omega_0)$.

For a Gaussian white noise, the correlator is $\langle \delta\varepsilon(t) \delta\varepsilon(t') \rangle = 2\Gamma_2 \delta(t - t')$. As $\delta\phi(t) = \int_0^t \delta\varepsilon(\tau) d\tau$, we take the average over noise in Eq. (3) using $\langle e^{i\delta\phi(t)} e^{-i\delta\phi(t')} \rangle = e^{-\Gamma_2 |t - t'|}$, with Γ_2 the decoherence (pure dephasing) rate for this model of classical diagonal noise.

The next step is to perform the time integration in Eq. (3), getting

$$W = \frac{\Delta^2 \Gamma_2}{2} \text{Re} \left\{ \sum_{nn'mm'} \lambda_{nn'mm'} \frac{e^{i(n-n')\alpha} e^{i\omega_0(n-n')t} e^{2i\omega_0(m'-m)t}}{[\varepsilon_0 + (2m-n)\omega_0]^2 + \Gamma_2^2} \right\}, \quad (5)$$

with $\lambda_{nn'mm'} \equiv J_n(x_1) J_{n'}(x_1) J_m(x_2) J_{m'}(x_2)$.

Under the fast driving regime, the nonzero exponents are highly oscillating compared to the time scale of the driving. Therefore, we only keep the contributions with $\omega_0(n - n') + 2\omega_0(m' - m) = 0$, and the transition rate reads

$$W = \frac{\Delta^2 \Gamma_2}{2} \sum_{nn'mm'} \frac{\lambda_{nn'mm'} \cos[(n - n')\alpha]}{[\varepsilon_0 + (2m - n)\omega_0]^2 + \Gamma_2^2} \delta_{n-n', 2(m-m')}. \quad (6)$$

Equation (6) exhibits an explicit dependence on the phase lag α , and a Lorentzian line shape close to the resonance condition $\varepsilon_0 = (n - 2m)\omega_0$, which is characteristic of white noise models in the regime of times $t \ll T_1$. For $x_2 = 0$, Eq. (6) reduces to the expression of the transition rate obtained for single driving protocols [26,29].

In Fig. 2 we plot $2W$ obtained from Eq. (6) as a function of the static flux detuning ε_0 , for the symmetric driving $\alpha = 0$ in Fig. 2(a) and for $\alpha = 0.2$ in Fig. 2(b). The parameters are $\Delta/h = 19$ MHz, $\omega_0/(2\pi) = 125$ MHz, $A_1 = 3m\Phi_0$, and $A_2 = 1.65m\Phi_0$, identical to those reported in the experiment of Ref. [12]. The salient feature is that the peaks are not symmetric with ε_0 , exhibiting a more fluctuating pattern of resonances for $\varepsilon_0 < 0$. This is a manifestation of the sensitivity of the total accumulated phase in one period of the driving with ε_0 and α . We have chosen the same amplitudes ratio $A_2/A_1 = 0.55$ as in Ref. [12], selected to drive the qubit up to four times through the avoided crossing in one driving period τ , in the range of negative detunings $\varepsilon_0 < 0$ (see Fig. 1). The strong fluctuating pattern is due to the three different phases (one phase for two successive passages) and eight possible superposition states that arise as ε_0 is varied. For other values of ε_0 , the waveform traverses the avoided crossing zero or two

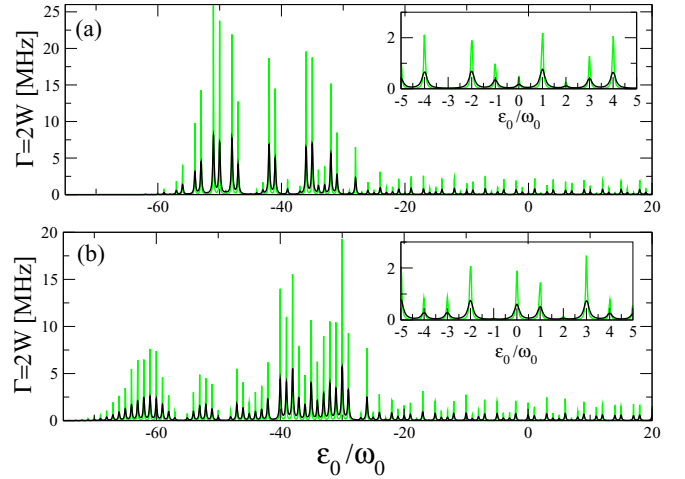


FIG. 2. Rate $2W$ obtained from Eq. (6) for parameters $\Delta/h = 19$ MHz, $\omega_0/(2\pi) = 125$ MHz, $A_1 = 3m\Phi_0$, $A_2 = 1.65m\Phi_0$, for $\Gamma_2 = 100$ MHz (black line) and $\Gamma_2 = 30$ MHz (green line). (a) $\alpha = 0$, (b) $\alpha = 0.2$. The insets show a magnification of selected resonances.

times per cycle, producing no accumulated phase or a single one, with interference conditions that originate a smoother behavior of Γ with ε_0 .

As expected, the resonance peaks decrease and turn wider as the dephasing rate Γ_2 , included in Eq. (6) as a parameter, is increased. This is fully consistent with the transition from the nonoverlapping to the overlapping resonances limit, also observed experimentally for the single harmonic driving protocols [10,14].

The derivation can be adapted to consider other spectral functions with Gaussian noise. In the case of FQs, the magnetic flux noise in SQUIDS could have a spectral density $S(\omega)$, which for low frequencies behaves as $1/\omega^p$ noise [28,29]. For this case, we get for the transition rate

$$\begin{aligned}
 W_{lf} &= \Delta^2 \sqrt{\frac{\pi}{8\Gamma_2}} \sum_{nn'mm'} \lambda_{nn'mm'} \cos[(n - n')\alpha] \\
 &\times \exp \left\{ \frac{-[\varepsilon_0 + (2m - n)\omega_0]^2}{\Gamma_2} \right\}, \quad (7)
 \end{aligned}$$

where $\Gamma_2 = \int S(\omega) d\omega$ is assumed finite, and we define W_{lf} as the transition rate induced by driven in the presence of low frequency noise. Notice that the main effect of a noise with a low frequency part is to modify the Lorentzian line shape of the individual resonances by a Gaussian line shape.

In Ref. [12], the transition rate induced by driving W was fully identified with the equilibration rate Γ (up to a factor 2). As we anticipated, this requires values $W < \Gamma_2$, and time scales $t \ll T_1 = 1/\Gamma_1$.

We will show in the next section that new characteristics emerge in the behavior of the equilibration rate when the full dynamics, including quantum noise, is considered within the Floquet-Born-Markov approach. In particular, we will analyze the behavior and sensitivity of the decoherence and relaxation rates with the flux detuning. The strong variations that these two rates experience, close to resonances with the driving field, question the results of this section for times scales close to full relaxation.

B. Equilibration rate within the Floquet-Born-Markov master equation

We start this section by reviewing the main ingredients of the Floquet-Born-Markov formalism, and for further details we suggest the Appendix of Ref. [22].

Since the system is driven with a biharmonic magnetic flux $f(t) = A_1 \cos(\omega_0 t + \alpha) - A_2 \cos(2\omega_0 t)$, the Hamiltonian is time periodic $\mathcal{H}(t) = \mathcal{H}(t + \tau)$, with $\tau = 2\pi/\omega_0$. In the Floquet formalism, which allows us to treat periodic forces of arbitrary strength and frequency [15,21,22,27], the solutions of the Schrödinger equation are of the form $|\Psi_\beta(t)\rangle = e^{i\mu_\beta t/\hbar} |\beta(t)\rangle$, where the Floquet states $|\beta(t)\rangle$ satisfy $|\beta(t)\rangle = |\beta(t + \tau)\rangle = \sum_k |\beta_k\rangle e^{-ik\omega_0 t}$, and are eigenstates of the equation $[\mathcal{H}(t) - i\hbar\partial/\partial t]|\beta(t)\rangle = \mu_\beta |\beta(t)\rangle$, with μ_β the associated quasienergy.

Experimentally, FQs are affected by the electromagnetic environment that introduces decoherence and relaxation processes. A standard theoretical model to cope with these effects is to linearly couple the system to a bath of harmonic oscillators with a spectral density $J(\omega)$ and equilibrated at temperature T [20,30–32]. For the FQs the dominating source of noise is fluxlike, in which case the bath degrees of freedom couple with the system variable φ_l [22,32]. In the two-level representation of Eq. (2), the flux noise is usually represented by a system bath Hamiltonian of the form $H_{sb} \propto \hat{\sigma}_z$ [30].

For weak coupling (Born approximation) and fast bath relaxation (Markov approximation), a Floquet-Born-Markov master equation for the reduced density matrix $\hat{\rho}$ in the Floquet basis, $\rho_{\alpha\beta}(t) = \langle \alpha(t) | \hat{\rho}(t) | \beta(t) \rangle$, can be obtained [20].

Considering that the time scale t_r for full relaxation satisfied $t_r \gg \tau$, one gets (see Appendix of Ref. [22] for details)

$$\frac{d\rho_{\alpha\beta}(t)}{dt} = -\frac{i}{\hbar}(\mu_\alpha - \mu_\beta)\rho_{\alpha\beta}(t) + \sum_{\alpha'\beta'} L_{\alpha'\beta'\alpha\beta} \rho_{\alpha'\beta'}(t). \quad (8)$$

The first term in Eq. (8) represents the nondissipative dynamics and the influence of the bath is described by the rate coefficients averaged over one period of the driving τ [22],

$$L_{\alpha\beta\alpha'\beta'} = R_{\alpha\beta\alpha'\beta'} + R_{\beta\alpha'\beta'\alpha}^* - \sum_{\eta} (\delta_{\beta\beta'} R_{\eta\eta\alpha'\alpha} + \delta_{\alpha\alpha'} R_{\eta\eta\beta'\beta}^*). \quad (9)$$

The rates

$$R_{\alpha\beta\alpha'\beta'} = \sum_q g_{\alpha\alpha'}^q A_{\alpha\alpha'}^q A_{\beta'\beta}^{-q} \quad (10)$$

can be interpreted as sums of q -photon exchange terms and contains information on the system-bath coupling operator $A_{\alpha\beta}^q = \sum_{nm} \sum_k \alpha_{k,n}^* \beta_{k+q,m} \langle n | \varphi_l | m \rangle$ written down in terms of the eigenbasis $|n\rangle$ of the Hamiltonian for the undriven case, Eq. (1), with $\alpha_{k,n} = \langle n | \alpha_k \rangle$. The nature of the bath is encoded in the coefficients $g_{\alpha\beta}^q = J(\mu_{\alpha\beta}^q/\hbar) n_{\text{th}}(\mu_{\alpha\beta}^q)$ with $\mu_{\alpha\beta}^q = \mu_\alpha - \mu_\beta + q\hbar\omega_0$ and $n_{\text{th}}(x) = 1/[\exp(x/k_B T) - 1]$. Here we consider FQs in contact with an Ohmic bath with a spectral density $J(\omega) = \gamma\omega$ (with a cutoff frequency), defining $J(-x) = -J(x)$ for $x < 0$, but other spectral densities could be included [22].

The Floquet-Born-Markov formalism has been extensively employed to study relaxation and decoherence in double-well

potentials and two-level systems driven by single frequency periodic evolutions [20,31,33–35]. More recently we applied it to analyze FQs under strong harmonic driving [21,22], when many energy levels have to be taken into account.

As in the present work, the dynamics of the FQs under a weak biharmonic driving protocol is studied, in the following the Hamiltonian will be reduced to its lowest two levels, Eq. (2).

For large times scales, it is usually assumed that the density matrix becomes approximately diagonal in the Floquet basis [31]. This approximation is justified when $\mu_\alpha - \mu_\beta \gg L_{\alpha'\beta'\alpha\beta}$, which is fulfilled for very weak coupling with the environment and away from resonances [22,34–36]. However, to compute fluctuation effects it is necessary to sweep in the dc flux detuning ϵ_0 , attaining near resonances quasidegeneracies, i.e., $\mu_\alpha - \mu_\beta \sim 0$. Therefore, as the dynamics of the diagonal and off-diagonal density matrix cannot be separated, we have to solve the full Floquet-Born-Markov equation [Eq. (8)] to find relaxation and decoherence rates close to resonances.

The rates are extracted from the nonzero eigenvalues of the matrix $\hat{\Lambda}$, given from its entries in the Floquet basis $L_{\alpha\beta\alpha'\beta'}$, defined in Eq. (9). The long time relaxation rate $\Gamma_r = 1/t_r$ is the minimum real eigenvalue (excluding the eigenvalue 0). In addition, the decoherence rate Γ_{ab} is given by the negative real part of the complex conjugate pairs of eigenvalues of $\hat{\Lambda}$ [22].

The sensitivity of both rates Γ_{ab} and Γ_r on the dc flux detuning and the driving amplitude has been analyzed in recent studies of the phenomena of population inversion and dynamic transitions in the LZS interference patterns of (single) driven FQs. Both phenomena emerge away from resonances, in the long time regime [21,22].

In addition, as we show below, close to resonances decoherence and relaxation rates we will attain values much larger than those predicted for the undriven case.

In Fig. 3, Γ_{ab} and Γ_r are plotted as a function of the normalized flux detuning ϵ_0/ω_0 —to visualize the resonances positions at integer values. The calculations were performed for the same parameters and driving protocol as in Fig. 2, and for an ohmic bath at $T = 20$ mK, which is the temperature reported in the experiment of Ref. [12].

Both rates exhibit a strong dependence with the detuning and important variations at resonances. In the case of the decoherence rate Γ_{ab} (Fig. 3 upper panel), although its value away from resonances is of the order of $\Gamma_{ab} \sim 100$ MHz—similar to the decoherence rate $1/T_2 = 100$ MHz in Ref. [12]; the important variations displayed at resonances redound in effectively doubling the reported decoherence time.

The rate Γ_r is plotted in the lower panels of Fig. 3 together with $2W$, computed from Eq. (6) for a constant value of the parameter $\Gamma_2 = 100$ MHz (green line), and for Γ_2 replaced by Γ_{ab} obtained within the FM formalism (red line), to include the dependence with the dc flux already described. The nominal values of $2W$ and Γ_r away from resonances are quite similar and even the positions of the resonances are well captured in both cases (see the lower panel for a blow up). However, at resonances Γ_r can attain values close to 100 MHz, satisfying $\Gamma_r \sim 2\Gamma_{ab}$. This is expected for a longitudinal system-bath coupling (as the one considered in the present work, i.e., $H_{sb} \propto \hat{\sigma}_z$) and is a fingerprint of the suppression of a pure dephasing mechanism on resonance

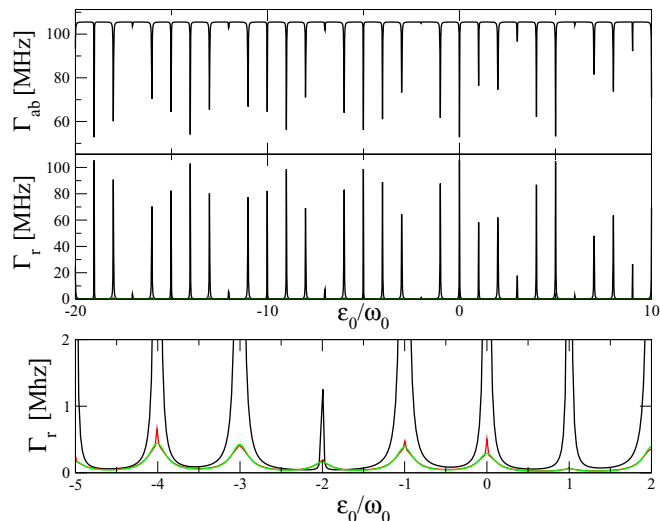


FIG. 3. Upper panel: Decoherence rate Γ_{ab} obtained in the FM formalism, as a function of the normalized flux detuning ϵ_0/ω_0 . Intermediate panel: Relaxation rate Γ_r as a function of (normalized) flux detuning obtained within the FM formalism (black solid line). Rate $2W$ obtained from Eq. (6) with $\Gamma_2 = 100$ MHz (green line) and after replacing $\Gamma_2 \rightarrow \Gamma_{ab}$ (red line). The lower panel shows an enlarged view to stress the differences between Γ_r and $2W$ close to resonances. Parameters are $\Delta/h = 19$ MHz, $\omega_0/(2\pi) = 125$ MHz, $A_1 = 3m\Phi_0$, and $A_2 = 1.65m\Phi_0$. For the FM calculations the bath is ohmic, $J(\omega) = \gamma\omega$, at temperature $T = 20$ mK with coupling $\gamma = 0.001$.

condition [22,31]. Notice that when $\Gamma_r \sim 2\Gamma_{ab}$ the time scale separation $T_1 \gg T_2$ —which was assumed in the experiment of Ref. [12] and in the phenomenological approach developed in Sec. III A—is not fulfilled.

Although the resonance condition could seem very sharp to be experimentally fulfilled, significant increments in the values of Γ_r relative to the background values can also be appreciated in a close vicinity, as it is displayed in Fig. 4(a).

Relative changes of $\sim 10\%$ – 20% in ϵ_0/ω_0 produce concomitant variations in the values of Γ_r which give rise to different profiles for the associated excited state occupation probabilities $P_+(t)$ [see Fig. 4(b)]. Even for time scales $t \sim t_{\text{expt}} \sim 1000\tau$, appreciable differences still persist in the respective $P_+(t_{\text{expt}})$.

IV. COMPUTING AVERAGES AND FLUCTUATIONS IN THE RATES: THE MESOSCOPIC ANALOGY

The total accumulated phase during the driving protocol is controlled by the asymmetry parameter α , which modifies the biharmonic waveform. As a consequence, $2W$ and Γ_r should experience, besides the sensitivity on ϵ_0 , fluctuations as a function of α [12].

As we already mentioned, the transition rate induced by the driving W was identified in Ref. [12] with an effective transition amplitude—the essential ingredient to determine the conductance in the Landauer formalism [1]. Under the assumption that the equilibration rate can be written as $\Gamma = 2W$, the approach was to associate the fluctuations in Γ as function of the dc flux, with the universal conductance

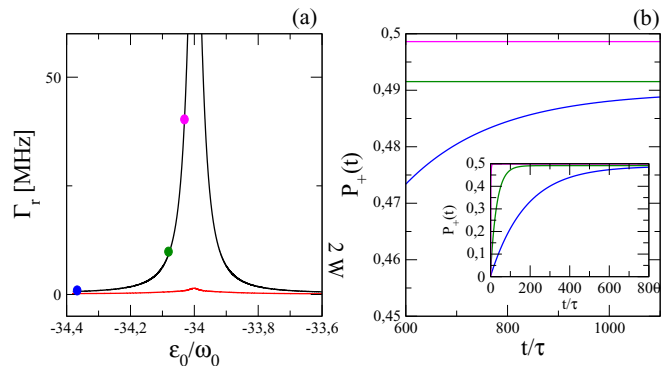


FIG. 4. (a) Relaxation rates Γ_r close to a resonance obtained within the FM formalism as a function of the normalized flux detuning ϵ_0/ω_0 and for the same parameters as in Fig. 3. The red curve corresponds to $\Gamma = 2W$ obtained from Eq. (6), after replacing $\Gamma_2 \rightarrow \Gamma_{ab}$. The chosen resonance corresponds to $\epsilon_0/\omega_0 = -34$. (b) Excited state occupation probability $P_+(t)$ as a function of the normalized time t/τ , obtained for three sampled values of Γ_r [identified by the dots in (a)]. In each case, the initial state is the ground state of the TLS Hamiltonian Eq. (2) for the correspondent flux detuning ϵ_0/ω_0 .

fluctuations (UCF), in analogy with mesoscopic electronic systems [2].

In the previous section, we have seen that for time scales close to full relaxation and around resonances with the driving field, important and quantitative differences emerge between $2W$ and the relaxation (equilibration) rate Γ_r obtained within the FM formalism. Associated with this, the respective fluctuation patterns will also exhibit different behaviors, as we show in the following.

The averages $\langle 2W \rangle$ and $\langle \Gamma_r \rangle$, over ϵ_0 , are defined as $\langle \dots \rangle = \frac{1}{\epsilon^{\text{max}}} \int_0^{\epsilon^{\text{max}}} \dots d\epsilon_0$, and play the role of ensemble averages over different scatterers configurations. In the case of the phenomenological approach we computed from Eq. (6):

$$\begin{aligned} \langle W \rangle &= \frac{\Delta^2}{2\epsilon^{\text{max}}} \sum_{nn'mm'} \lambda_{nn'mm'} \cos[(n-n')\alpha] \\ &\times \left[\arctan\left(\frac{(2m-n)\omega_0}{\Gamma_2}\right) - \arctan\left(\frac{(2m-n)\omega_0 - \epsilon^{\text{max}}}{\Gamma_2}\right) \right] \end{aligned} \quad (11)$$

and

$$\langle W^2 \rangle = \frac{1}{\epsilon^{\text{max}}} \int_0^{\epsilon^{\text{max}}} W^2 d\epsilon_0. \quad (12)$$

Although $\langle W^2 \rangle$ does not have a simple analytic expression, its numerical evaluation is straightforward. The fluctuations in $2W$ are defined as $\sigma_{2W} = 2\sqrt{\langle W^2 \rangle - \langle W \rangle^2}$.

In the case of the relaxation rate Γ_r , its average $\langle \Gamma_r \rangle$ and fluctuations σ_r have been computed numerically.

In Fig. 5(a) we plot the averaged rates relative to its values at $\alpha = 0.5$, i.e., $\langle \Gamma_r \rangle_n \equiv \langle \Gamma_r \rangle / \langle \Gamma_r \rangle_{(\alpha=0.5)}$ and $\langle 2W \rangle_n \equiv \langle 2W \rangle / \langle 2W \rangle_{(\alpha=0.5)}$, in order to establish a fair comparison for different bath temperatures, couplings γ , or dephasing rates Γ_2 , respectively.

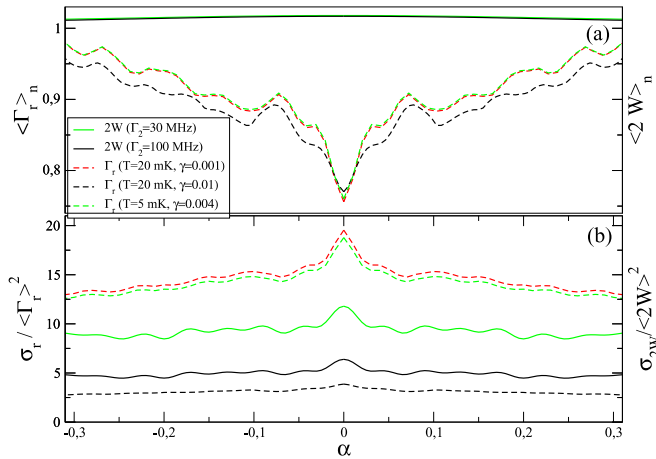


FIG. 5. Normalized rates $\langle \Gamma_r \rangle_n$ and $\langle 2W \rangle_n$ (a) and normalized standard deviations $\sigma_r / \langle \Gamma_r \rangle_n^2$ and $\sigma_{2W} / \langle 2W \rangle_n^2$ (b) averaged from $-4m\Phi_0$ to $0m\Phi_0$ as a function of the time reversal broken parameter α . The different values of the dephasing rate Γ_2 used to compute $\Gamma = 2W$ and the values of the temperature T and bath coupling constant γ employed to compute the rates Γ_r within the FM formalism are, respectively, specified in the inset. System parameters are $\Delta/h = 19$ MHz, $\omega_0/(2\pi) = 125$ MHz, $A_1 = 3m\Phi_0$, and $A_2 = 1.65m\Phi_0$.

Even after performing the averages in flux detuning, strong fluctuations are still visible as a function of α . Notice that $\langle 2W \rangle_n$ is almost independent of α and the dephasing rate Γ_2 , in agreement with the results of Ref. [12]. On the other hand, $\langle \Gamma_r \rangle_n$ exhibit a sharp dip at $\alpha = 0$, that could be interpreted as the fingerprint of the WL correction—in analogy to the correction present in the quantum conductance of mesoscopic disordered systems [3]. The relative fluctuations (normalized to the squared mean values) are defined as $\sigma_r / \langle \Gamma_r \rangle_n^2$ and $\sigma_{2W} / \langle 2W \rangle_n^2$, and are plotted in Fig. 5(b). The profiles resemble the UCF found in short mesoscopic wires, with the fluctuations at $\alpha = 0$ enhanced compared to the fluctuations for $\alpha \neq 0$, as the theory of UCF predicts when the time reversal symmetry is broken [2].

The WL correction and the UCF tend to wash out as either the effective temperature and/or the coupling with the environment are increased, as expected when decoherence and relaxation processes become more efficient. This is clearly observed in Figs. 5(a) and 5(b). In addition, the profiles remain almost undisturbed when the product of the effective temperature T times the bath coupling γ remains constant, although each one is varied separately. This is consistent with the well known result that the dominant contribution to the decoherence rate depends on the product γT [32].

We want to point out some limitations of the phenomenological approach employed in Sec. III A and followed in Ref. [12]. On one hand, it disregards relaxation assuming that the equilibration rate Γ is given by $2W$. As a consequence, the equilibration rates are largely underestimated close to resonances, as we emphasized when describing Fig. 3. On the other hand, the interpretation of Γ as a conductance is only well justified away from resonances, when it is satisfied that $\Gamma \sim 2W$.

Last but not least, we want to comment on the detection of the WL effect, which has not been measured in Ref. [12]. To our view the limitation which precludes the experimental observation of the WL-like effect is not the driving protocol, as the authors of Ref. [12] suggested, but mainly the difficulty in capturing the extremely sharp resonant conditions as the flux detuning is swept, and also the relatively short experimental decoherence times T_2 . From the theory of disordered electronic systems it is known that the size of the weak localization correction scales (logarithmically) with the dephasing time $\tau_\phi \propto T_2$ [3].

Consistent with this result, Fig. 5(a) shows very well defined dips in $\langle \Gamma_r \rangle_n$ at $\alpha = 0$, for values of the coupling $\gamma = 0.004$ – 0.001 and temperature of 20 mK—as reported experimentally. These values give decoherence rates $\Gamma_2 \sim 25$ – 30 MHz ($T_2 = 1/\Gamma_2 \simeq 30$ – 40 ns). Thus it is expected that for slightly larger values of T_2 —but not so far from the reported $T_2 \sim 10$ ns, it could be possible to experimentally access the full WL dip, once the resonance conditions can be explored.

V. CONCLUSIONS AND PERSPECTIVES

In this work we have tested fluctuation effects associated with broken time reversal symmetry in FQs driven by a biharmonic (dc + ac) magnetic flux with a phase lag.

Employing the full Floquet-Born-Markov master equation we have computed relaxation Γ_r and decoherence Γ_{ab} rates, both strongly dependent on the phase lag and the dc flux detuning, exhibiting appreciable fluctuations. As a function of the dc flux and away from the resonance conditions with the driving field $\Gamma_{ab} \rightarrow \Gamma_2$ and $\Gamma_r \rightarrow \Gamma_1$ with $\Gamma_2 = 1/T_2 \gg \Gamma_1 = 1/T_1$, i.e., in agreement with the relaxation and decoherence rates predicted for the undriven FQs. However, close to resonances both rates take values which differ significantly from the respective ones away from resonances, even satisfying $2\Gamma_{ab} \sim \Gamma_r$.

The relaxation (equilibration) rate Γ_r can be accessed experimentally by measuring the decay of the flux qubit excited state population. Recently the fluctuations in the measured equilibration rate have been analyzed and associated with universal conductance fluctuations (UCFs), following an analogy to well known phenomena exhibited in disordered mesoscopic electronic systems [12]. However, as we discuss in the extent of this work, the *mesoscopic analogy* is only well justified for the out of resonance regime, when the equilibration rate can be described in terms of a transition probability induced by the driving protocol.

Besides UCF, we also predict that the WL effect can be detected for the biharmonic driving protocol. However, to observe this effect, the experiments should be performed in a more coherent regime, in which larger values of T_2 could be attained. Nowadays the control on the environmental bath degrees of freedom is a promising way to enlarge coherence, as have been recently proposed and tested [21,37,38].

By increasing the driving amplitude, the multilevel structure of the FQs could be explored and more avoided crossings could be reached. This regime of strong driving seems to be experimentally attainable, as the amplitude spectroscopy experiments for the biharmonic drive [39] have proven. On the theoretical side, it would be interesting to extend the

calculations of the fluctuations for the multilevel structure of the FQs in order to explore the mesoscopic analogy, beyond the weak scattering limit studied in the present work.

Last but not least, it should be mentioned that protocols of biharmonic drive in qubits coupled to a transmission-line resonator, double quantum dots, NV-centers, and cold atoms, have been recently studied experimentally [40,41] and theoretically [42–48]. These artificial atoms are also potential qubits to test our predictions.

ACKNOWLEDGMENTS

We acknowledge support from Comisión Nacional de Energía Atómica, Gobierno de Argentina, Universidad Nacional de Cuyo (06/ C455), Consejo Nacional de Investigaciones Científicas y Técnicas (PIP11220150100218, PIP11220150100327), and Agencia Nacional de Promoción Científica y Tecnológica (PICT2011-1537, PICT2014-1382).

-
- [1] S. Datta, *Electronic Transport in Mesoscopic Systems* (Cambridge University Press, Cambridge, 1995).
- [2] A. Benoit, C. P. Umbach, R. B. Laibowitz, and R. A. Webb, *Phys. Rev. Lett.* **58**, 2343 (1987); S. Washburn and R. A. Webb, *Rep. Prog. Phys.* **55**, 1311 (1992).
- [3] G. Bergmann, *Phys. Rev. B* **25**, 2937(R) (1982); D. J. Bishop, R. C. Dynes, and D. C. Tsui, *ibid.* **26**, 773 (1982).
- [4] E. Akkermans, G. Montambaux, J. L. Pichard, and J. Zinn-Justin, *Mesoscopic Quantum Physics* (Elsevier, Amsterdam, 1994).
- [5] J. E. Mooij, T. P. Orlando, L. S. Levitov, L. Tian, C. H. van der Wal, and S. Lloyd, *Science* **285**, 1036 (1999); T. P. Orlando, J. E. Mooij, L. Tian, C. H. van der Wal, L. S. Levitov, S. Lloyd, and J. J. Mazo, *Phys. Rev. B* **60**, 15398 (1999).
- [6] I. Chiorescu, Y. Nakamura, C. J. P. M. Harmans, and J. E. Mooij, *Science* **299**, 1869 (2003).
- [7] J. Diggins, R. Whiteman, T. D. Clark, R. J. Prance, H. Prance, J. F. Ralph, A. Widom, and Y. N. Srivastava, *Physica B* **233**, 8 (1997).
- [8] M. J. Everitt, T. D. Clark, P. Stiffell, H. Prance, R. J. Prance, A. Vourdas, and J. F. Ralph, *Phys. Rev. B* **64**, 184517 (2001).
- [9] M. J. Everitt, P. Stiffell, T. D. Clark, A. Vourdas, J. F. Ralph, H. Prance, and R. J. Prance, *Phys. Rev. B* **63**, 144530 (2001).
- [10] W. D. Oliver, Y. Yu, J. C. Lee, K. K. Berggren, L. S. Levitov, and T. P. Orlando, *Science* **310**, 1653 (2005).
- [11] J. Q. You and F. Nori, *Nature (London)* **474**, 589 (2011).
- [12] S. Gustavsson, J. Bylander, and W. D. Oliver, *Phys. Rev. Lett.* **110**, 016603 (2013).
- [13] A. Ferrón and D. Domínguez, *Phys. Rev. B* **81**, 104505 (2010).
- [14] D. M. Berns, M. S. Rudner, S. O. Valenzuela, K. K. Berggren, W. D. Oliver, L. S. Levitov, and T. P. Orlando, *Nature (London)* **455**, 51 (2008); W. D. Oliver and S. O. Valenzuela, *Quantum Inf. Process* **8**, 261 (2009).
- [15] A. Ferrón, D. Domínguez, and M. J. Sánchez, *Phys. Rev. B* **82**, 134522 (2010).
- [16] Y. Nakamura, Y. A. Pashkin, and J. S. Tsai, *Phys. Rev. Lett.* **87**, 246601 (2001); M. Sillanpää, T. Lehtinen, A. Paila, Y. Makhlin, and P. Hakonen, *ibid.* **96**, 187002 (2006); C. M. Wilson, T. Duty, F. Persson, M. Sandberg, G. Johansson, and P. Delsing, *ibid.* **98**, 257003 (2007).
- [17] M. Mark, T. Kraemer, P. Waldburger, J. Herbig, C. Chin, H.-C. Nägerl, and R. Grimm, *Phys. Rev. Lett.* **99**, 113201 (2007).
- [18] P. Huang, J. Zhou, F. Fang, X. Kong, X. Xu, C. Ju, and J. Du, *Phys. Rev. X* **1**, 011003 (2011).
- [19] G. Sun *et al.*, *Appl. Phys. Lett.* **94**, 102502 (2009).
- [20] S. Kohler, T. Dittrich, and P. Hänggi, *Phys. Rev. E* **55**, 300 (1997); S. Kohler, R. Utermann, P. Hänggi, and T. Dittrich, *ibid.* **58**, 7219 (1998).
- [21] A. Ferrón, D. Domínguez, and M. J. Sánchez, *Phys. Rev. Lett.* **109**, 237005 (2012).
- [22] A. Ferrón, D. Domínguez, and M. J. Sánchez, *Phys. Rev. B* **93**, 064521 (2016).
- [23] S. N. Shevchenko, S. Ashhab, and F. Nori, *Phys. Rep.* **492**, 1 (2010).
- [24] E. Dupont-Ferrier, B. Roche, B. Voisin, X. Jehl, R. Wacquez, M. Vinet, M. Sanquer, and S. De Franceschi, *Phys. Rev. Lett.* **110**, 136802 (2013).
- [25] A. Ferrón, D. Domínguez, and M. J. Sánchez, *J. Phys.: Conf. Ser.* **568**, 052028 (2014).
- [26] D. M. Berns, W. D. Oliver, S. C. Valenzuela, A. V. Shytov, K. K. Berggren, L. S. Levitov, and T. P. Orlando, *Phys. Rev. Lett.* **97**, 150502 (2006).
- [27] J. H. Shirley, *Phys. Rev.* **138**, B979 (1965).
- [28] E. Paladino, Y. M. Galperin, G. Falci, and B. L. Altshuler, *Rev. Mod. Phys.* **86**, 361 (2014).
- [29] M. H. S. Amin and D. V. Averin, *Phys. Rev. Lett.* **100**, 197001 (2008).
- [30] M. C. Goorden, M. Thorwart, and M. Grifoni, *Phys. Rev. Lett.* **93**, 267005 (2004); *Eur. Phys. J. B* **45**, 405 (2005).
- [31] J. Hausinger and M. Grifoni, *Phys. Rev. A* **81**, 022117 (2010).
- [32] C. H. van der Wal *et al.*, *Eur. Phys. J. B* **31**, 111 (2003); G. Burkard, R. H. Koch, and D. P. DiVincenzo, *Phys. Rev. B* **69**, 064503 (2004).
- [33] M. Grifoni and P. Hänggi, *Phys. Rep.* **304**, 229 (1998).
- [34] H.-P. Breuer, W. Huber, and F. Petruccione, *Phys. Rev. E* **61**, 4883 (2000).
- [35] D. W. Hone, R. Ketzmerick, and W. Kohn, *Phys. Rev. E* **79**, 051129 (2009).
- [36] S. Gasparinetti, P. Solinas, S. Puggnetti, R. Fazio, and J. P. Pekola, *Phys. Rev. Lett.* **110**, 150403 (2013).
- [37] J. Paavola and S. Maniscalco, *Phys. Rev. A* **82**, 012114 (2010).
- [38] Z. Chen, J. Kelly, C. Quintana, R. Barends, B. Campbell, Yu Chen, B. Chiaro, A. Dunsworth, A. G. Fowler, E. Lucero, E. Jeffrey, A. Megrant, J. Mutus, M. Neeley, C. Neill, P. J. J. O'Malley, P. Roushan, D. Sank, A. Vainsencher, J. Wenner, T. C. White, A. N. Korotkov, and J. M. Martinis, *Phys. Rev. Lett.* **116**, 020501 (2016).
- [39] J. Bylander, M. S. Rudner, A. V. Shytov, S. O. Valenzuela, D. M. Berns, K. K. Berggren, L. S. Levitov, and W. D. Oliver, *Phys. Rev. B* **80**, 220506(R) (2009).

- [40] F. Forster, M. Mühlbacher, R. Blattmann, D. Schuh, W. Wegscheider, S. Ludwig, and S. Kohler, *Phys. Rev. B* **92**, 245422 (2015).
- [41] M. Yan, E. G. Rickey, and Y. Zhu, *Phys. Rev. A* **64**, 013412 (2001).
- [42] A. M. Satanin, M. V. Denisenko, A. I. Gelman, and F. Nori, *Phys. Rev. B* **90**, 104516 (2014).
- [43] S. N. Shevchenko, G. Oelsner, Ya. S. Greenberg, P. Macha, D. S. Karpov, M. Grajcar, U. Hübner, A. N. Omelyanchouk, and E. Il'ichev, *Phys. Rev. B* **89**, 184504 (2014).
- [44] R. Blattmann, P. Hänggi, and S. Kohler, *Phys. Rev. A* **91**, 042109 (2015).
- [45] L. Yatsenko and H. Metcalf, *Phys. Rev. A* **70**, 063402 (2004).
- [46] C. L. Garrido Alzar, H. Perrin, B. M. Garraway, and V. Lorent, *Phys. Rev. A* **74**, 053413 (2006).
- [47] A. P. Saiko and R. Fedaruk, *JETP Lett.* **91**, 681 (2010).
- [48] A. P. Saiko, R. Fedaruk, and S. A. Markevich, *J. Phys. B* **47**, 155502 (2014).